

Article

Balancing Water Ecosystem Services: Assessing Water Yield and Purification in Shanxi

Man Li ¹, Shanshan Li ¹, Huancai Liu ^{1,2,*} and Junjie Zhang ¹¹ School of Geographical Science, Shanxi Normal University, Taiyuan 030031, China² School of Geography and Tourism, Shaanxi Normal University, Shannxi 710062, China

* Correspondence: liuhc@sxnu.edu.cn

Abstract: Water yield and purification are important aspects of water ecosystem services, and achieving a balanced development of the two is necessary for the development of aquatic ecosystems. Using the InVEST model, the spatiotemporal variations of regional water yield and purification services in Shanxi, China, from 2000 to 2020 were analyzed. Three future scenarios (natural development, urban development, and ecological protection) were assessed for 2030 using the PLUS model. The results showed that in 2000–2020, the water yield of Shanxi Province in terms of space was generally low in the middle and northwest and high in the southeast, and it was affected by land-use change and climatic change. From 2000 to 2020, the water yield of Shanxi Province changed by 78.8 mm. In 2030, water yield will be highest under the urban development scenario (380.53 mm) and lowest in the ecological protection scenario (368.22 mm). Moreover, the water quality purification capacity improved, with nitrogen loading high in the center and low in the east and west. Due to the implementation of environmental protection policies and the improvement of the technical level, the nitrogen load was the highest in 2000 (0.97 kg/hm²) and lowest in 2015 (0.94 kg/hm²). By 2030, because of the high nitrogen loadings of cultivation and construction land and low nitrogen loadings of forests and grasslands, the nitrogen load was lowest under the scenario of urban development (0.94 kg/hm²) and highest under ecological protection (0.85 kg/hm²).

Keywords: water yield; water purification services; InVEST model; PLUS model; Shanxi Province

Citation: Li, M.; Li, S.; Liu, H.; Zhang, J. Balancing Water Ecosystem Services: Assessing Water Yield and Purification in Shanxi. *Water* **2023**, *15*, 3261. <https://doi.org/10.3390/w15183261>

Academic Editors: Micòl Mastrocicco, Bin He, Quanhua Hou and Ahmed Elbeltagi

Received: 4 August 2023

Revised: 9 September 2023

Accepted: 12 September 2023

Published: 13 September 2023



Copyright: © 2023 by the authors. Licensee MDPI, Basel, Switzerland. This article is an open access article distributed under the terms and conditions of the Creative Commons Attribution (CC BY) license (<https://creativecommons.org/licenses/by/4.0/>).

1. Introduction

Water ecosystem services reflect the ability of ecosystems to process and regulate water and can provide guarantees for water resources and environmental security for human society [1]. With the increase in socioeconomic development, human demand for water resources has become increasingly intense, leading to frequent water shortages, water pollution, and severe impacts on the sustainable development of the region [2–4]. Since the 18th National Congress of the Communist Party of China (CPC), as the construction of ecological civilization has been integrated into social and economic construction, the evaluation of ecosystem service capacity has become increasingly important [5]. The balanced development between water yield and purification is of great significance for maintaining the stability, biodiversity, sustainable use, and healthy development of human society [6–8].

With the development of Geographic Information Systems and remote sensing technologies in ecology and hydrology, many models and methods can be used to simulate regional water yield and purification services [9–11]. For example, models such as the DHI MIKE, Topography-based Hydrological Model, Soil and Water Assessment Tool (SWAT), Terrain Lab, and Integrated Valuation of Ecosystem Services and Tradeoffs (InVEST) have been used to simulate and analyze water yield services in different watersheds; models or methods such as the single-factor method, Nemero index method, grey evaluation method, SWAT, DO concentrations, the support vector regression (SVR) model, and InVEST have been used to evaluate water quality conditions in different regions [12,13].

The InVEST model is an open-source ecosystem service function assessment model based on the ecological production process, assessment, and trade-off of ecosystem services. It calculates the physical and value quantities of ecosystem services, incorporates socioeconomic factors into ecosystem conservation decisions, and enables the spatial presentation of ecosystem services.

Owing to fewer parameter requirements [14–16], flexible parameter adjustments, a wide range of applications [17], and other advantages, the InVEST model is widely used by scholars and has achieved good results. However, the model has limitations, such as high data dependence, parameterization and calibration challenges, and the complexity of economic valuation. Internationally, Redhead et al. [18], Daneshi et al. [19], and Bejagam et al. [20], respectively, used the InVEST model to simulate the water yield of the British rivers, the basin flowing into the Caspian Sea in northern Iran, and the Tungabhadra basin in the Indian peninsula. In China, Li et al. [21], Chen et al. [22], and Li et al. [23], respectively, used the InVEST model to analyze the spatial and temporal changes in water resources and water ecosystem services in Shaanxi Province, Hanjiang City, and Taihu Lake Basin. In Shanxi, Pan et al. [24], Wang et al. [25], and Yang et al. [26] used the InVEST model to analyze the spatiotemporal evolution of coalfield ecosystem services in Shanxi Province, the pattern of multiple ecosystem services and ecological security in Shanxi Province, and the coupling and coordination of the sustainable development of the ecosystem in Shanxi Province. However, there are fewer assessments of water ecosystem services in Shanxi Province. The geographical location and ecological environment of Shanxi Province are extremely important. Therefore, it is very important to supplement the research on the water ecological environment in Shanxi Province.

To more accurately predict future changes in water ecosystem services, scholars have performed a large number of studies on the possibility of future land-use change [27,28], among which the Patch-generating land-use simulation (PLUS) model is widely used because of its high simulation accuracy, fast data processing, and effective simulation of complex land-use evolution. The PLUS model has been used to predict the land-use and ecosystem services of water ecosystems. Currently, combining the prediction of multi-scenario land-use and ecosystem services has become a popular topic in research. Ferreira et al. [29] provided suggestions for future ecological restoration in the southwestern region of Portugal by predicting the land-use status of the region. Gao et al. [30] analyzed the future ecological risk status of the local ecosystems by predicting the land-use types of Nanjing for 2025 under multiple future scenarios. Li et al. [31] predicted the land-use types and assessed the carbon stock in Kunming City based on the PLUS and InVEST models to provide a reference for mitigating regional carbon loss.

Located in the eastern part of the Loess Plateau and the middle reaches of the Yellow River, Shanxi Province is an important economic and ecological region in China and a vital part of the Yellow River Basin [32]. It is situated at the northern boundary of the East Asian summer wind system. This geographic location exposes the province to the dynamic interplay of mid-latitude westerly winds and Asian monsoon winds [33]. The territory is crisscrossed by mountains and has a complex topography; its unique geographic location and elevation make it a sensitive area to climate change [34]. In Shanxi Province, an important energy and chemical base in China, industrial water consumption is high and causes serious water pollution. The degradation of aquatic ecosystem services has long been a prominent concern [35]. The quality of the water ecological environment in Shanxi Province can directly affect the fragile ecological environment and country of Shanxi Province in terms of the development of the people's economy. As an important water yield area in the Yellow River Basin, it will also be related to the water resources situation of the entire Yellow River Basin.

Quantitative research on water yield and purification in Shanxi Province is essential for government departments to understand the production, distribution, and utilization of water resources, which is conducive to the rational planning for the allocation and utilization of such resources. Such research can help better understand the health status of

water ecosystems in Shanxi Province and provide a scientific basis for ecological protection and restoration, thereby contributing to improving the quality of water bodies and reducing the impact of water pollution on ecology and human health, helping the government formulate reasonable development strategies, balancing the relationship between economic growth and environmental protection, and achieving sustainable social, economic, and environmental development [36].

In this study, we conducted a quantitative assessment using the InVEST model to analyze the spatiotemporal variations in water yield and purification services from 2000 to 2020. Additionally, three future development scenarios (natural development, urban development, and ecological protection) were established to estimate the potential water yield and purification services in 2030. This research seeks to provide scientific support for the sustainable development of regional aquatic ecosystems, with a particular emphasis on the importance of maintaining the co-development between water quantity and quality to ensure ecological preservation.

2. Methodology

2.1. Study Area

Shanxi Province (34°34′–40°44′ N, 110°14′–114°33′ E) in North China has a total area of 15.67×10^4 km² (Figure 1). This area comprises various landforms, such as mountains, hills, plateaus, and basins. Mountains and hills account for 80% of the total area of the province; the terrain is high in the northeast and low in the southwest. It has a temperate continental monsoon climate and an uneven seasonal distribution of precipitation, with more precipitation in summer and fall and less precipitation in winter and spring. Shanxi Province spans two major water systems, the Yellow and Hai Rivers, with a total annual average water resource of 180.59×10^8 m³, of which the Yellow River Basin includes the basins of the Fen, Yellow Tributary, Sushui, and Qin Rivers; and the Hai River Basin includes the basins of the Yongding, Hutuo, Zhangwei, and Daqing Rivers.

2.2. Data Sources

This study mainly utilized spatial data, including meteorological, natural environment, soil, socioeconomic, land-use, and road information data (Table 1). Owing to the different resolutions of these data sources, the necessary data were resampled and projected by raster processing. The spatial resolution of all data was standardized to 30 m by ArcMap10.7, and the coordinate system used was Krasovsky_1940_Albers.

Table 1. Data sources and descriptions.

Categorization	Data Type	Data Sources and Processing
Meteorological elements	Measured quantity of rain	Data Center for Resource and Environmental Sciences, Chinese Academy of Sciences (http://www.resdc.cn)
	Temperatures	
	Potential evapotranspiration	National Meteorological Information Center-China Meteorological Data Network (http://www.cma.cn)
Natural environment	DEM	Geospatial Data Cloud (http://www.gscloud.cn)
	Slope	Calculated from DEM data in ArcGIS to get
Soil features	Soil data	Chinese soil information in the World Soil Database (HWSD)
Socioeconomic	GDP	Data Center for Resource and Environmental Sciences, Chinese Academy of Sciences (http://www.resdc.cn)
	Demographic	
Land use	Land-use type	

Table 1. Cont.

Category	Data Type	Data Sources and Processing
Road information	Distance to the first level of road	National Geographic Information Resources Catalog Service System (http://www.servicetianditu.gov.cn)
	Distance to secondary roads	
	Distance to tertiary roads	
	Distance to highway	
	Distance to railroad	
	Distance to Government	

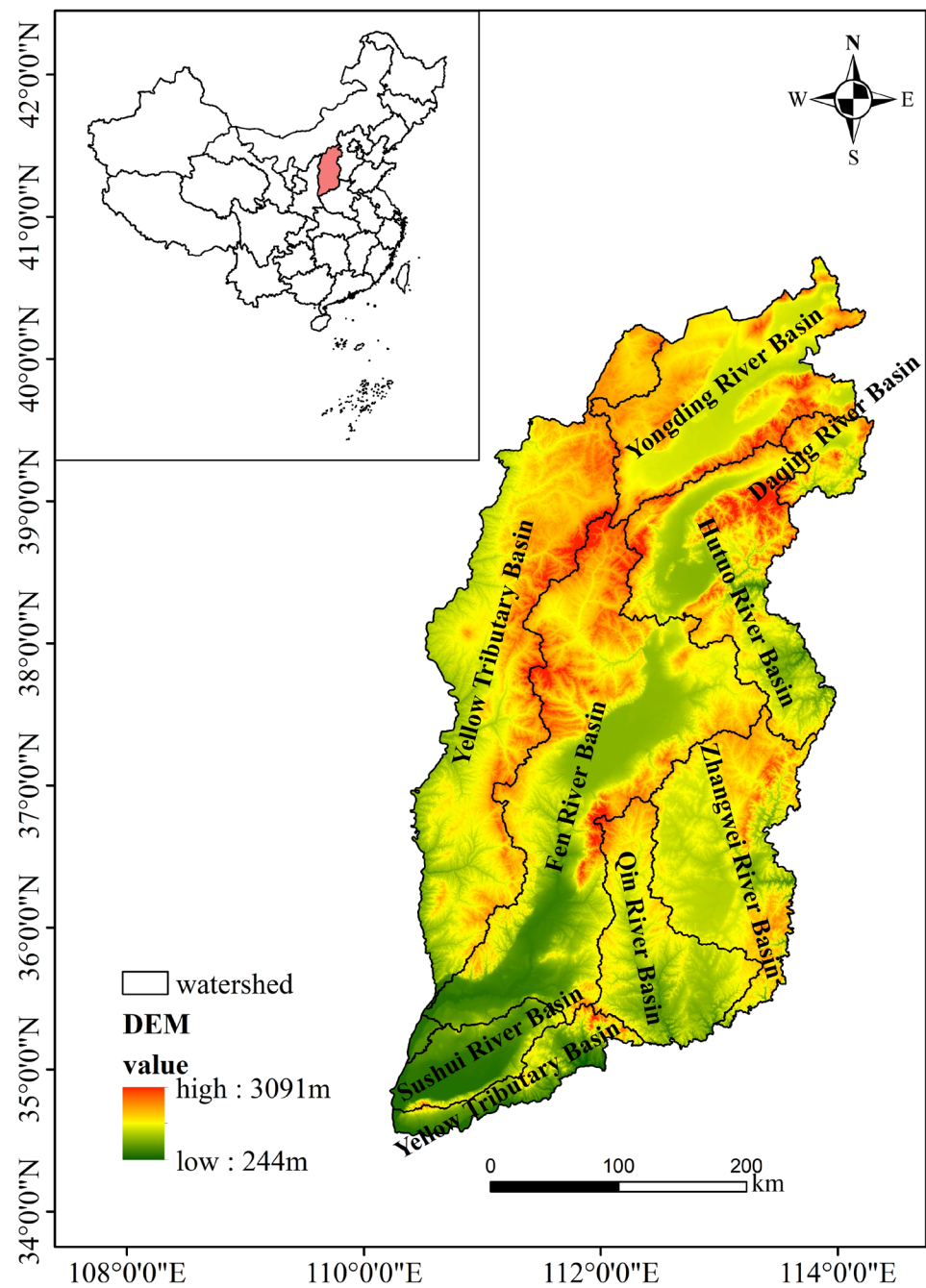


Figure 1. Overview of the geographic location of Shanxi Province.

2.3. Research Methodology

2.3.1. InVEST Model

The InVEST model is an ecosystem assessment model based on different surface land covers that can be used to simulate the material quality and quantity of ecosystem services and spatialize ecosystem services to improve natural resource management. The model includes multiple submodules, such as water yield, water purification, soil conservation, and habitat quality. For the evaluation of aquatic ecosystem services in Shanxi Province in this study, water yield and purification modules were mainly utilized to calculate the amount of water yield and nitrogen loading. The details of the modules used are as follows:

(1) Water yield module

The water yield module (water yield) is an estimation method based on the water balance method and Budyko's water-heat balance assumption [37], which combines meteorological, topographic, vegetation, soil, and other data, using the difference between precipitation and evapotranspiration to obtain the water yield. The greater the water yield, the greater the water supply. This study compared the impact of land-use changes on water yield under different scenarios for 2020 and 2030, where the water yield in 2030 was based on precipitation in 2020. The calculation formula is as follows:

$$Y(x) = \left(1 - \frac{AET(x)}{p(x)}\right) \cdot p(x) \quad (1)$$

$$\frac{AET(x)}{p(x)} = \frac{1 + w(x) + R(x)}{1 + w(x) \cdot R(x) + 1/R(x)} \quad (2)$$

$$w(x) = Z \cdot \frac{PAWC(x)}{p(x)} \quad (3)$$

$$R(x) = \frac{k(x) \cdot ET_0}{P(x)} \quad (4)$$

where $Y(x)$ is the average annual water yield (mm), $AET(x)$ is the average annual actual evapotranspiration (mm), $P(x)$ is the average annual precipitation (mm), $R(x)$ is the Budyko drying coefficient, and $PAWC(x)$ is the available water content of vegetation (mm), which is the coefficient of evapotranspiration of vegetation and the average annual reference evapotranspiration (mm). Z denotes the Zhang coefficient [38], which was obtained by improving the calculations based on the Budyko curve. Through continuous simulation improvement, when Z was 4.03, the difference between the simulated average annual water yield and actual natural runoff in Shanxi Province was the smallest, and the simulation results were the best.

(2) Water purification module

The nutrient retention module estimates the effect of vegetation and soil on water purification based on the ability of nitrogen nutrients in runoff to remove pollutants and determines the capacity of water purification. The higher the total nitrogen content, the more severe the pollution level of the watershed and the weaker the water quality purification capacity. The calculation formula is as follows:

$$ALV_x = HSS_x * pol_x \quad (5)$$

$$HSS_x = \frac{\lambda_x}{\bar{\lambda}_w} \quad (6)$$

$$\lambda_x = \log(\sum_u Y_u) \quad (7)$$

where ALV_x is the adjusted load value, pol_x is the output coefficient, HSS_x is the hydrological sensitivity score, λ_x is the runoff index, $\bar{\lambda}_w$ is the average runoff index in the watershed, and $\sum_u Y_u$ is the total water yield (mm) within the runoff path.

As different land-use types exhibit different water purification capacities, their biophysical coefficients are different. This study combined the results of relevant existing research to determine the local biophysical coefficients (Table 2) [39], which can be used to reflect the attributes of the soil cover and land-use types. This specifically includes the actual evapotranspiration assignment, root depth, plant evapotranspiration coefficients, nitrogen loading coefficients, nitrogen sequestration efficiency, and other relevant parameters. The actual evapotranspiration assignment was assigned as 1 and 0 based on whether there was vegetation cover or not, respectively.

Table 2. Details of biophysical coefficients.

Land-Use Type	Actual Evapotranspiration Assignment	Depth of Root System (mm)	Plant Evapotranspiration Coefficient	Nitrogen Load Factor	Nitrogen Interception Efficiency
Arable land	1	350	0.75	18.23	0.4
Woodland	1	2500	0.93	3.45	0.75
Grassland	1	750	0.63	8.02	0.5
Waters	0	1	1	0.01	0.05
Construction land	0	1	0.25	11.03	0.05
Unused land	1	20	0.4	9.83	0.05

2.3.2. Bivariate Spatial Correlation Model

Global spatial autocorrelation can describe the overall distribution of a phenomenon and determine whether the phenomenon has agglomeration characteristics in space; however, it cannot precisely identify the areas in which local spatial autocorrelation can project the scope of the agglomeration [40]. Among these, the Geoda tool can analyze raster spatial data, which can effectively reveal the correlation between different elements of spatial units, and the calculation formulas are as follows:

$$\text{Moran's } I = \frac{N \sum_i \sum_{j \neq i} W_{ij} z_i^a z_j^b}{(N-1) \sum_i \sum_{j \neq i} W_{ij}} \quad (8)$$

$$\text{LISA}_i = \frac{1}{N} \frac{(x_i - \bar{x})}{\sum_i (x_i - \bar{x})^2} \sum_j W_{ij} (x_j - \bar{x}) \quad (9)$$

where Moran's I denotes the bivariate global Moran's index, z_i^a is the deviation of the attribute of the i th cell from the mean, W_{ij} is the spatial weight matrix, and N is the number of units in the study area. The value of Moran's I is in the range of -1 to 1 ; Moran's $I > 0$, < 0 , and $= 0$ indicate positive, negative, and no correlations, respectively. Local indicators of spatial association (LISA) is the bivariate local autocorrelation index, where x_i is the attribute value of unit i and represents the average of all attribute values. When $\text{LISA} > 0$, the spatial cell is a high-high- or low-low-value spatial agglomeration, and when $\text{LISA} < 0$, the spatial cell is a high-low- or low-high-value spatial agglomeration.

2.3.3. PLUS Model

The PLUS model is a recently developed model that is based on traditional land-use simulation and random forest models such as system dynamics [41], Future Land-Use Simulation [42], CLUE-Scanner [43], and Spatial-temporal Markov chain [44] models. It integrates a Create-a-Research-Space model of a multi-type random seed mechanism that can be used to analyze the drivers of land expansion and predict the evolution of land-use patches.

To evaluate the simulation accuracy, the simulated land-use types in 2020 were compared with real land-use data in 2020. The Kappa coefficient was found to be 0.84, which was greater than 0.7, indicating its high simulation accuracy. Therefore, it can be used to predict the land-use types in Shanxi Province by 2030.

Land use is affected by policies, economic development, natural environment, and other aspects. Due to the uncertainty of future development, it is based on the land use changes in Shanxi Province from 2000 to 2020 and the possibility of future development under three future development scenarios (i.e., natural development, urban development, and ecological protection). Simulations and projections of changes in land use in Shanxi Province by 2030 were then developed. These three development scenarios are designed to explore more comprehensively the impacts of land use on ecosystems. These different scenarios are set up for several reasons: the natural development scenario takes into account natural evolution and natural processes and helps to understand the impact of land use on aquatic ecosystems in the absence of human policy interventions; the urban development scenario takes into account that Shanxi Province is in the rising stage of economic transformation, and urban expansion may still exist in the future; the ecological protection scenario takes into account that the environmental awareness of the government and the public is gradually rising, and in order to achieve the sustainable and high-quality development of Shanxi Province, ecological protection measures may be strengthened in the future. Under the natural development scenario, the change in each land-use type continues the current development trend; under the urban development scenario, the transfer of construction land to other land-use types is restricted, but other land can be transferred to construction land; and under the ecological protection scenario, the transfer of ecological land, such as woodland, grassland, and water, to other land is restricted, but other land can be transferred to ecological land types (Table 3; where “+” indicates transferable and “−” indicates non-transferable land).

Table 3. Multi-scenario land-use transfer matrix.

Scenario Setting	Land-Use Type	Arable Land	Woodland	Grassland	Waters	Construction Land	Unused Land
Natural Development scenario	Arable land	+	−	+	+	−	+
	Woodland	−	+	+	−	−	+
	Grassland	+	+	+	+	−	+
	Waters	−	−	+	+	−	+
	Construction Land	+	−	+	−	+	+
	Unused land	+	+	+	+	−	+
Urban Development Scenario	Arable land	+	+	+	−	−	+
	Woodland	−	+	−	+	+	+
	Grassland	−	−	+	+	+	+
	Waters	−	−	−	+	−	+
	Construction Land	+	+	+	+	+	+
	Unused land	+	+	−	−	−	+
Ecological Protection Scenario	Arable land	+	−	−	−	−	+
	Woodland	+	+	+	−	−	+
	Grassland	+	−	+	−	−	+
	Waters	+	−	+	+	−	+
	Construction Land	+	−	−	−	+	+
	Unused land	+	−	−	−	−	+

3. Results and Discussion

3.1. Changes in Water Yield in Shanxi Province from 2000 to 2020

3.1.1. Temporal Variations

Generally, water yield is mainly affected by rainfall and actual evapotranspiration, whereas the main factors affecting actual evapotranspiration include air temperature and land use [45]. In Shanxi Province, the differences in the average water yield of different land-use types were as follows: unutilized land > constructed land > grassland > cultivated land > woodland > waters. Because most unutilized land is not shaded by vegetation or artificial structures, this allows precipitation to directly reach the surface, whereas the

hardened surface of the constructed land makes it difficult for precipitation to infiltrate. The average multi-year water yield of unutilized and constructed land reached 295.44 and 234.29 mm, respectively.

Grassland, arable land, and woodland exhibited medium water yield capacities. Although grassland was vegetated, water evaporation was relatively low, and the root system was shallow, with an average water yield of 214 mm. Arable land was usually artificially managed and improved, and the root systems of crops were more developed; therefore, it absorbed and utilized the water in the soil more efficiently, with an average water yield of 217.69 mm. Because woodland had exuberant branches and leaves with high evapotranspiration, the formation of a layer of withered material and humus on the surface played a positive role in water conservation, with an average water yield of 220.25 mm. Waters, despite being a storage space for water, were unable to absorb and utilize water, and the average water yield was 151.40 mm.

The water yield in Shanxi Province from 2000 to 2020 showed an N-shaped change, characterized by a small increase, then a decline and a subsequent increase (Figure 2). The average water yield in Shanxi Province in 2000 was 297.01 mm, and the high-value areas of water yield were mainly located in the Qin, Zhangwei, and Hutuo River Basins in the eastern part of Shanxi, owing to their abundant precipitation. However, 2015 was a very strong El Niño year; the province's precipitation was only 480.60 mm, the average temperature was 1 °C higher than normal, and, therefore, the water yield was low at only 265.27 mm. In contrast, 2020 was the subsequent year of El Niño, when the rainfall reached $877.2 \times 10^8 \text{ m}^3$, with an average rain depth of 561.3 mm; thus, the year had a biased abundance of water [46]. Meanwhile, with the rapid development of the local society and economy and the popularization and implementation of the policy of "returning farmland to forests," the expansion of construction land has occupied a large amount of arable land and grassland. Furthermore, the increase in construction land from 2000 to 2020 was 106.22%, which has greatly increased the area of impermeable layers. Consequently, the average water yield of the province in 2020 reached 375.80 mm, which was higher than that of 2000 and 78.79 mm higher than the average water yield in 2000.

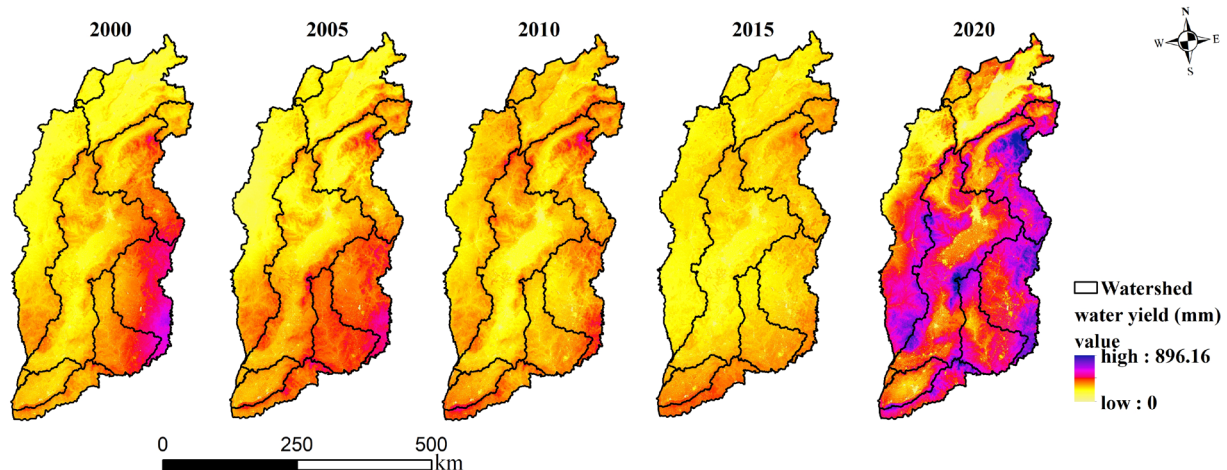


Figure 2. Water yield in Shanxi Province from 2000 to 2020.

3.1.2. Spatial Variations

Water yield is greatly influenced by climate and human activities. Affected by this, it shows the spatial differentiation characteristics are generally low in the middle and northwest and high in the southeast in terms of space (Table 4). The water yield in the central basin area is low, the topography of the basin is usually surrounded by surrounding mountains or mountains, and water replenishment is limited. Moreover, the basin's topography has a high rate of evaporation and transpiration because the surrounding mountains block the wind, making it possible for the humidity to increase, resulting in

more evaporation and transpiration of water. In the northern region, Datong and Xinzhou had mines, and to ensure the dryness of the mines and associated workspaces, a large amount of groundwater was extracted, which led to the destruction of underground aquifers, a continuous decrease in water yield, and, thereby, a negative impact on the local water ecosystem. This encouraged the local area to actively promote the mine's ecological restoration and, thereby, the benign development of the regional ecology. The water yield in the western part of Shanxi Province is low, mainly because most of the area belongs to the arid climate zone, with a dry climate and lack of sufficient precipitation. The western region has high and complex terrain, more mountainous areas, and poor water storage conditions. The ecological environment in the western region is poor, and problems such as soil erosion are serious, affecting the maintenance and supply of water resources. In recent years, the Lvliang Mountain area has experienced abundant precipitation and vigorous vegetation growth. With the popularization of soil and water conservation projects, water-saving technology, and other measures, the high water yield area has shifted from the southeastern part of the Haihe River Basin to the Lvliang Mountain area in the Yellow River Basin.

Table 4. Water yield in different watersheds in Shanxi Province (all units in mm).

Watershed	Year	2000	2005	2010	2015	2020
Yellow River Basin	Fen River Basin	278.9	291.27	268.68	245.49	385.57
	Yellow Tributary Basin	281.75	300.44	315.34	298.05	362.45
	Sushui River Basin	281.44	319.17	321.27	327.17	335.06
	Qin River Basin	370.53	406.94	304.93	289.52	403.08
Sea River Basin	Yongding River Basin	213	233.73	283.2	250.43	267.09
	Hutuo River Basin	333.32	287.5	310.45	284.99	427.41
	Zhangwei River Basin	441.03	404	314.29	276.73	435.6
	Daqing River Basin	300.44	326.42	341.76	320.76	401.76

Located in the eastern part of Shanxi Province, the Haihe River Basin generally has a high level of urbanization, and land use is dominated by construction and industrial land, with an average annual water yield of 322.70 mm. The Zhangwei, Hutuo, and Daqing River Basins are situated on the windward slopes of the Taihang Mountain System, with high precipitation and low evaporation, with an average annual water yield of 328.73–374.33 mm.

The Yellow River Basin in the central and western parts of Shanxi Province is a semi-arid region, with land-use types dominated by cropland and grassland and an average water yield of only 319.35 mm. The Fen and Sushui River Basins are located on the leeward slopes of the Taihang and Taiyue Mountains, with topography dominated by basins, high temperatures, and strong evapotranspiration; their average water yields are 293.98 and 316.82 mm, respectively.

3.2. Spatiotemporal Variation in Water Purification Services in Shanxi Province from 2000 to 2020

The ability to remove nitrogen can be used to reflect the ability to purify water, and different land types have different abilities to absorb and remove nitrogen. Studies have shown that the annual average nitrogen loads of various land-use types are in the following order: cropland > construction land > unutilized land > grassland > woodland > waters. In agricultural activities, some pesticides and fertilizers are not absorbed by crops, which accumulate nitrogen on the surface, leading to a nitrogen load in the croplands of Shanxi Province of 1.64 kg/hm². During the urbanization process, a large amount of nitrogen oxides is generated from energy consumption, industrial production, and transportation, which is deposited into water bodies in the form of acid rain, and some enterprises directly discharge nitrogen-containing wastewater into the water bodies; this increased the nitrogen loading of construction land in Shanxi Province to 0.99 kg/hm². Because forests and grasslands have strong nitrogen-fixing capacities, their nitrogen loads were lower. In water, aquatic plants and plankton can absorb and utilize nitrogen in the water, whereas the water

body can dilute the nitrogen via water flow and circulation. Consequently, the nitrogen load in the water bodies of Shanxi Province was only 0.01 kg/hm².

The nitrogen load in Shanxi Province is affected by a variety of factors, including agriculture, industry, urbanization, and the natural environment. Therefore, spatially, the nitrogen loading in Shanxi Province was high in the central part and low in the eastern and western parts (Figure 3). Areas with low water purification capacities were mainly distributed in the south-central part of the Yellow River Basin, the northern part of the Haihe River Basin, and the southeastern part of Shanxi Province. A large amount of discharged urban and industrial sewage and applied chemical fertilizers increased the nitrogen load and lowered the water purification capacity in the province. Areas with higher water purification capacities were mainly distributed in the southeastern part of the Yellow River Basin and the Lvliang Mountain area, which are mountainous and hilly, with large forest and grassland distributions.

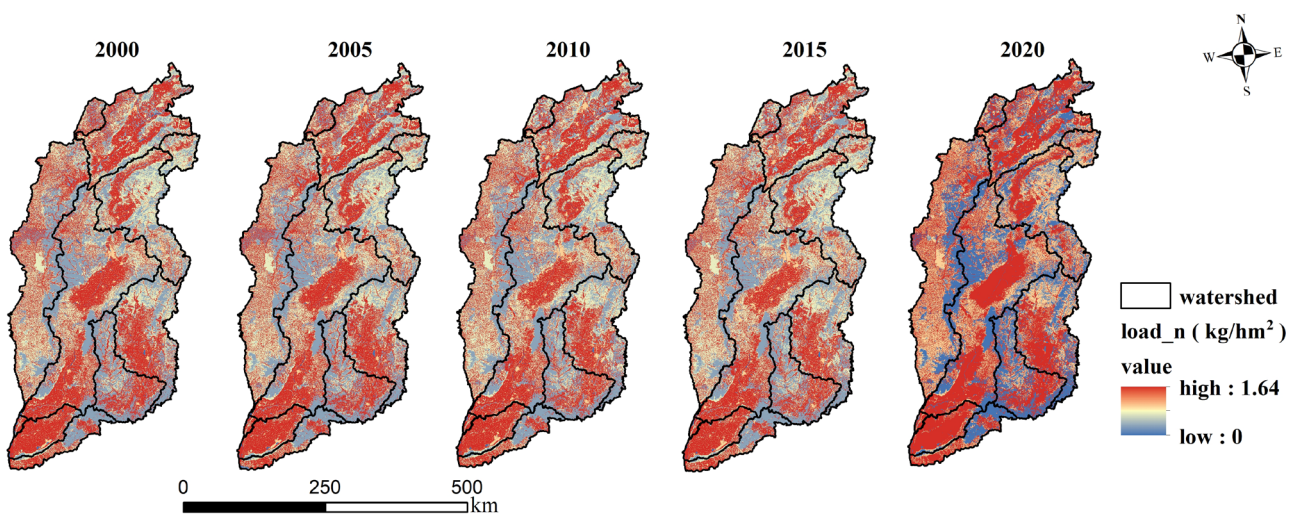


Figure 3. Nitrogen output load from 2000 to 2020.

During 2000–2020, the water purification capacity of the Haihe and Yellow River Basins increased overall. Among them, with the implementation of environmental protection and “returning farmland to forest” policies, the area with higher water purification capacity expanded significantly in the Lvliang Mountain area of the Yellow River Basin; however, in the central area of the Fen River Basin, owing to the increasing level of urbanization and subsequent increase in regional nitrogen loading, the areas with low water purification capacity are expanding into the north-central part of the Fenhe River Basin.

3.3. Spatial Matching Analysis of Water Yield and Purification Services

Based on the Geoda spatial analysis tool, a spatial weight matrix was established, and the bivariate global Moran’s I index for water yield and purification services in Shanxi Province was calculated (Table 5). The results show that a significant and expanding trade-off occurred between water yield and water purification services during 2000–2020.

Table 5. The global Moran’s I index for water yield and water purification services.

Norm	2000	2005	2010	2015	2020
Moran’s I	−0.201	−0.204	−0.273	−0.216	−0.335
p-value	0.002	0.003	0.005	0.004	0.003

Analyzing the local spatial heterogeneity between water yield and purification services in Shanxi Province (Figure 4) revealed that the Hutuo River Basin, Zhangwei River Basin, southern part of the Yellow Tributary, and Fen River Basin were mainly “high-low”

agglomeration areas. This region had abundant precipitation that was distributed across forested grasslands, and it currently represents the optimal area for water ecology in Shanxi Province.

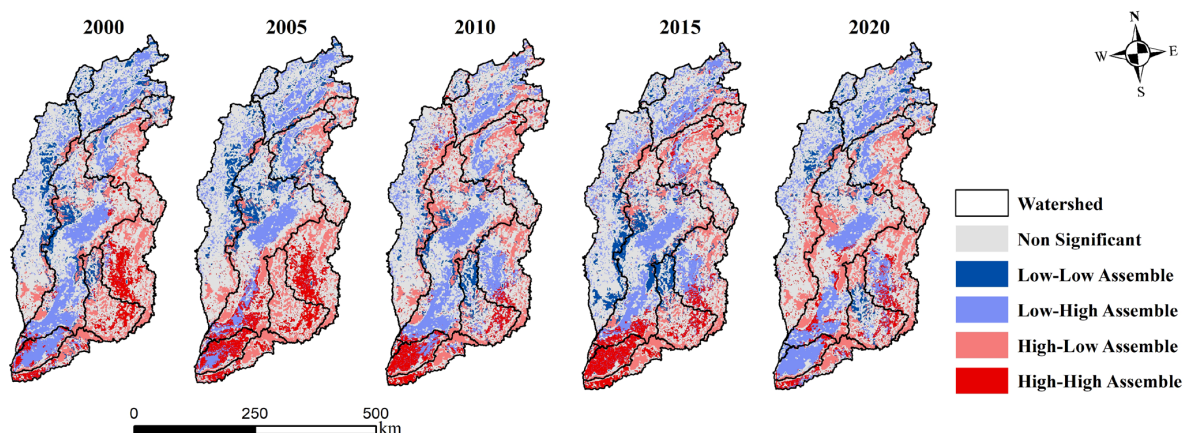


Figure 4. Bivariate local indicators of spatial association clustering of water yield and purification services in Shanxi Province.

The “low-high” agglomeration areas were mainly found to be distributed in the south-central part of the Yellow River Basin and the northern part of the Haihe River Basin, with high temperatures, high evaporation rates, and an abundance of arable land; this area is currently a low-value area for the quality of the water ecosystem in Shanxi Province. Under the influence of the increasing trend of local warming and drying, the significant increase in fertilizer application, and the uncontrolled discharge of nitrogen-containing wastewater, the “low-high” agglomeration area has a clear tendency to expand to the western part of the Zhangwei River Basin; therefore, special attention should be paid to the protection of the aquatic ecology in this area.

The “high-high” agglomeration areas were mainly distributed in the southern part of the Yellow River Basin and the southwestern part of the Haihe River Basin in Shanxi Province, where the arable land is widely spread and has rich precipitation, exhibiting high water yield and weak water purification capacity. However, over the past 20 years, with the promotion of the policy of returning farmland to forests, the local water purification capacity has been significantly improved, and “high-high” agglomeration areas have been decreasing.

The “low-low” agglomeration areas were mainly distributed in the eastern part of the basin of the tributaries of the Yellow River and the western part of the Qin River Basin, which are relatively small in area but have large forest and grassland distributions, and the vegetation has a strong ability to intercept precipitation. Notably, with the increase in precipitation in the Lvliang Mountain area, the local area showed a tendency to shift from the “low-low” catchment area to the “high-low” agglomeration area.

3.4. Characterization of Water Yield and Purification Services under Different Scenarios for 2030

By predicting the changes in water yield and nitrogen loading under the three scenarios (i.e., natural development, urban development, and ecological protection) for 2030, the following findings were obtained (Table 6).

Table 6. Average annual water yield and nitrogen loading in Shanxi Province from 2000 to 2020, and projections for 2030 under different scenarios.

Ecosystems/Year	2000	2005	2010	2015	2020	Natural Development	Urban Development	Ecological Protection
Water yield (mm)	297.01	299.39	294.06	265.27	375.81	372.19	380.53	368.22
Nitrogen loading (kg/hm ²)	0.97	0.96	0.95	0.94	0.95	0.91	0.94	0.85

Under the natural development scenario, Shanxi Province will continue with the development trend of the current land-use type. By 2030, the water yield capacity will change minimally, only 372.19 mm, which is slightly lower than that in 2020. Under the urban development scenario, construction land will be restricted from shifting to other land-use types but other land-use types can be transformed into construction land; therefore, by 2030, the area of construction land will have significantly increased compared with that of the other scenarios, whereas ecological land areas will decrease significantly, resulting in a water yield of 380.53 mm, a 1.3% increase compared with that in the year 2020. Under the ecological protection scenario, ecological environmental protection will be particularly emphasized by the government, which will lead to a significant increase in the area of ecological forests and grasslands, thereby increasing the intercepting capacity of vegetation for precipitation and increasing pollutants. The amount of water produced by 2030 is projected to decrease by 7.59 mm compared with that recorded in 2020.

With urban socioeconomic development and the improvement of wastewater treatment levels, the water purification capacity of Shanxi Province under the three scenarios will be higher in 2030 than it was in 2020, but the water purification capacities will be different under the different scenarios. The nitrogen loading under the natural development scenario will be 0.91 kg/hm², a decrease of 4.21% compared with that recorded in 2020. Under the urban development scenario, the nitrogen loading will be evidently higher than those in the other scenarios because of the significant increase in the area of construction land and the significant decrease in the areas of forest and grassland, which have strong absorption and removal capacities for nitrogen. Under the ecological protection scenario, the area of ecological forest and grassland will increase, and the ecological forest meadow will have an increased capacity to intercept pollutants and reach the water body. The capacity of the pollutants will be enhanced, and the nitrogen load reaching the water body is anticipated to decrease by 10.52%, or 0.85 kg/hm², compared with that recorded in 2020.

4. Conclusions and Discussion

4.1. Conclusions

Based on the InVEST model water yield and water purification module, the spatiotemporal changes in water yield and water purification in Shanxi Province from 2000 to 2020 and the correlation between the two were analyzed. Water yield and nitrogen loading under the three scenarios of natural development, urban development, and ecological protection by 2030 were predicted using the PLUS model. The results of this article are as follows:

1. The differences in the average water yield of the different land-use types in Shanxi Province were as follows: unutilized land > constructed land > grassland > cultivated land > woodland > waters. Temporally, the water yield of Shanxi Province from 2000 to 2020 can be characterized by an N shape. Affected by land-use change and climatic change, the lowest water yield (265.27 mm) occurred in 2015, and the highest (375.80 mm) was in 2020, showing a change of 110.53 mm; from 2000 to 2020, the water yield of Shanxi Province changed by 78.8 mm. Spatially, the water yield mainly exhibited characteristics of low spatial differentiation in the middle and northwest and high spatial differentiation in the southeast.
2. The water purification capacities of different land-use types were as follows: arable land > construction land > unutilized land > grassland > woodland > waters. Spatially, the areas with lower water purification capacities were mainly distributed in the south-central part of the Yellow River Basin and the northern and southeastern parts of the Haihe River Basin, whereas those with higher water purification capacities were mainly distributed in the southeastern part of the Yellow River Basin as well as in the Lvliangshan Mountain area. Due to the implementation of environmental protection policies and the improvement of the technical level, the nitrogen load was the highest (0.97 kg/hm²) in 2000 because of its large arable land area and high usage

- rate of pesticide fertilizers. In contrast, the nitrogen load was the lowest in 2015 (0.94 kg/hm²).
3. From 2000 to 2020, a significant and expanding trade-off occurred between the water yield and water purification services in Shanxi Province. The Hutuo River Basin, Zhangwei River Basin, southern part of the Yellow Tributary Basin, and Fenhe River Basin were primarily “high-low” agglomeration areas. The “low-high” agglomeration areas were mainly distributed in the south-central part of the Yellow River Basin and the northern part of the Haihe River Basin.
 4. By 2030, the urban development scenario yielded the most water (380.53 mm), whereas the ecological protection scenario yielded the least (368.22 mm). With urban socioeconomic development and sewage treatment level improvement, the water purification capacity of Shanxi Province in 2030 is expected to be higher than that in 2020 under all three scenarios; however, the ecological protection scenario had the strongest purification capacity, with a nitrogen load of only 0.85 kg/hm². In contrast, the urban development scenario had the weakest purification capacity (nitrogen load: 0.94 kg/hm²).

4.2. Discussion

The results show that the land-use type in the study area under the natural development scenario develops along the historical benchmark, reflecting the changes in the water ecological environment under current conditions, thereby having a minimal impact on the water ecological environment. Under the urban development scenario, the research area focuses on economic development and urban construction. The water yield and nitrogen load change the most; hence, urban expansion should be reasonably controlled, and ecological land should be protected [47,48]. The water ecological environment of Shanxi Province is ideal under the ecological protection scenario, but economic growth becomes relatively slow. Therefore, optimizing land use, increasing investment in sewage treatment science and technology, using pesticides and fertilizers rationally, and implementing river basin zoning are necessary for economic development. Science and technology must be used to promote the construction of ecological civilization, ensure the safety of the water ecological environment in the river basin, and improve the water ecological environment.

In this study, the spatiotemporal changes and correlation between water yield and purification services in Shanxi Province from 2000 to 2020 were investigated. We chose 5 years as a time node; although this reflects the changes in regional water ecology in time and space, this may cause some spatiotemporal information on water yield and water purification to be omitted. Moreover, both precipitation and land-use changes can affect the water yield capacity of a region. As this study focused on analyzing the impact of land-use change on water yield capacity, future precipitation was assumed to remain unchanged. The three development scenarios were simulated to provide a certain reference for the rational adjustment of the land-use types and protection. In future studies, the dual impacts of precipitation and land use can be considered and combined with the representative concentration pathway and shared socioeconomic pathway scenarios proposed in CMIP6 to comprehensively predict changes in water yield and purification capacity in Shanxi and other similar critical regions.

Relevant studies have shown that warming and drying trends in the climate in Shanxi Province will become increasingly prominent in the future [49,50]. Shanxi Province should consider ecological, social, and economic factors when formulating relevant policies and action plans and seek the best balance to achieve comprehensive sustainability:

1. In the context of agricultural production, areas with low water yield in Shanxi Province, such as the Fenhe River Basin and the Sushui River Basin, should promote the popularization of water-saving technologies such as sprinkler and drip irrigation, improve the efficiency of water resource utilization, and optimize water resource management systems. Areas with wide agricultural distribution and low water purification capacity, such as the central and southern regions of the Yellow

- River Basin, should also reduce the use of synthetic pesticides and chemical fertilizers and support organic agriculture.
2. In the context of ecosystem protection, areas with poor soil and water conservation, such as the cities of Jinzhong, Lvliang, and Yuncheng, should protect ecological forest belts (soil and water conservation forests), strengthen wind and sand control forests to reduce soil erosion and maintain soil moisture and nutrients, and protect water sources (wetlands, lakes, and rivers).
 3. In the context of urban development, areas with a high level of urbanization, such as the cities of Taiyuan, Datong, and Changzhi, should rationally control the scale of urban construction to reduce the discharge of nitrogenous sewage. Sewage treatments should be strengthened, and the scale of use of reclaimed water should be expanded.

Author Contributions: Conceptualization, M.L. and S.L.; data curation, S.L.; formal analysis, S.L.; funding acquisition, M.L. and H.L.; project administration, M.L. and H.L.; resources, S.L.; software, S.L.; investigation, S.L.; visualization, J.Z.; writing—original draft, S.L.; writing—review and editing, M.L. and H.L. All authors have read and agreed to the published version of the manuscript.

Funding: This research was funded by the Natural Science Research Project of Shanxi Province (202103021224258), and the Key subject of Shanxi Federation of Social Sciences (SSKLZDKT2023036).

Data Availability Statement: Not applicable.

Acknowledgments: We thank the editors and reviewers for reviewing this article and look forward to your valuable comments on this article.

Conflicts of Interest: The authors declare no conflict of interest. The funders had no role in the design of the study; in the collection, analyses, or interpretation of data; in the writing of the manuscript; or in the decision to publish the results.

References

1. Liu, J.; Li, J.; Qin, K. Changes in land-uses and ecosystem services under multi-scenarios simulation. *Sci. Total Environ.* **2017**, *586*, 522–526. [[CrossRef](#)]
2. Deng, X.; Zhao, C. Identification of Water Scarcity and Providing Solutions for Adapting to Climate Changes in the Heihe River Basin of China. *Adv. Meteorol.* **2014**, *2014*, 279173. [[CrossRef](#)]
3. Li, Y.; Mi, W.; Ji, L.; He, Q.; Yang, P.; Xie, S.; Bi, Y. Urbanization and agriculture intensification jointly enlarge the spatial inequality of river water quality. *Sci. Total Environ.* **2023**, *878*, 162559. [[CrossRef](#)] [[PubMed](#)]
4. Ban, Y.; Liu, X.; Yin, Z.; Li, X.; Yin, L.; Zheng, W. Effect of urbanization on aerosol optical depth over Beijing: Land use and surface temperature analysis. *Urban Clim.* **2023**, *51*, 101655. [[CrossRef](#)]
5. Chen, J.C.; Zhao, Z.; Wang, J.Y. Research on the essence and practical significance of the “Two Mountains Theory”. *For. Econ.* **2020**, *42*, 3–13. [[CrossRef](#)]
6. Bojie, F.; Guoyi, Z.; Yongfei, B.; Changchun, S.; Jiyuan, L.; Huiyuan, Z.; Yihe, L.; Hua, Z.; Gaodi, X. Functions and ecological security of major terrestrial ecosystems in China. *Prog. Earth Sci.* **2009**, *24*, 571–576.
7. Dai, E.; Wang, X.; Zhu, J. Progress and trend prospect of ecosystem service trade-off/synergy research. *Adv. Earth Sci.* **2015**, *30*, 1250–1259.
8. Costanza, R.; Darge, R.; Groot, R. The value of the world’s ecosystem services and natural capital. *Nature* **1997**, *387*, 253–260. [[CrossRef](#)]
9. Zhang, B.; Li, W.H.; Xie, G.D.; Xiao, Y. Water conservation function and measurement method of forest ecosystem. *J. Ecol.* **2009**, *28*, 6.
10. Cheng, X.; Chen, L.; Sun, R. An improved export coefficient model to estimate non-point source phosphorus pollution risks under complex precipitation and terrain conditions. *Environ. Sci. Pollut. Res.* **2018**, *25*, 20946–20955. [[CrossRef](#)]
11. Xie, Y.C.; Gong, J.; Qi, S.S. Spatial-temporal differentiation of water supply services in Bailongjiang River Basin based on InVEST model. *J. Nat. Resour.* **2017**, *32*, 1337–1347. [[CrossRef](#)]
12. Aryal, S.K.; Ashbolt, S.; Mcintosh, B.S. Assessing and Mitigating the Hydrological Impacts of Urbanisation in Semi-Urban Catchments Using the Storm Water Management Model. *Water Resour. Manag.* **2016**, *30*, 5437–5454. [[CrossRef](#)]
13. Nong, X.; Lai, X.; Chen, L.; Shao, D.; Zhang, C.; Liang, J. Prediction modelling framework comparative analysis of dissolved oxygen concentration variations using support vector regression coupled with multiple feature engineering and optimization methods: A case study in China. *Ecol. Indic.* **2023**, *146*, 109845. [[CrossRef](#)]
14. Wang, W.; Chen, L.; Shen, Z. Dynamic export coefficient model for evaluating the effects of environmental changes on non-point source pollution-Science Direct. *Sci. Total Environ.* **2020**, *747*, 141164. [[CrossRef](#)]

15. Zhang, F.P.; Li, X.J.; Feng, Q. Water conservation in the upper reaches of Heihe River Basin based on InVEST model. *Chin. Desert* **2018**, *38*, 9.
16. Ran, C.; Wang, S.; Bai, X. Trade-Offs and Synergies of Ecosystem Services in Southwestern China. *J. Environ. Eng. Sci.* **2020**, *37*, 669–678. [[CrossRef](#)]
17. Gao, J.; Li, F.; Gao, H. The impact of land-use change on water-related ecosystem services: A study of the Guishui River Basin, Beijing, China. *J. Clean. Prod.* **2015**, *163*, S148–S155. [[CrossRef](#)]
18. Redhead, J.W.; Stratford, C.; Sharps, K. Empirical validation of the InVEST water yield ecosystem service model at a national scale. *Sci. Total Environ.* **2016**, *569–570*, 1418–1426. [[CrossRef](#)] [[PubMed](#)]
19. Daneshi, A.; Brouwer, R.; Najafinejad, A. Modelling the impacts of climate and land use change on water security in a semi-arid forested watershed using InVEST. *J. Hydrol.* **2021**, *593*, 125621. [[CrossRef](#)]
20. Bejagam, V.; Keesara, V.R.; Sridhar, V. Impacts of climate change on water provisional services in Tungabhadra basin using InVEST Model. *River Res. Appl.* **2021**, *38*, 106–194. [[CrossRef](#)]
21. Li, Y.L.; He, Y.; Liu, W.Q.; Jia, L.P.; Zhang, Y.R. Evaluation and Prediction of Water Yield Services in Shaanxi Province, China. *Forests* **2023**, *14*, 229. [[CrossRef](#)]
22. Chen, Z.Y.; Yu, P.H.; Chen, Y.Y. Spatial-temporal evolution of water production and water purification services in the Han River Basin under shared socio-economic pathway. *Chin. J. Eco-Agric.* **2021**, *29*, 1800–1814. [[CrossRef](#)]
23. Li, Z.B.; Tao, Y.; Ou, W.X. Research on the relationship between supply and demand of aquatic ecological services in Taihu Lake Basin and multi-scenario assessment based on water quantity and water quality. *Acta Ecol. Sin.* **2023**, *5*, 2088–2100. [[CrossRef](#)]
24. Pan, H.H.; Wang, J.Q.; Du, Z.Q.; Wu, Z.T.; Zhang, H.; Ma, K.M. Spatiotemporal evolution of ecosystem services and its potential drivers in coalfields of Shanxi Province, China. *Ecol. Indic.* **2023**, *148*, 110109. [[CrossRef](#)]
25. Wang, J.; Li, Y.; Wang, S.; Li, Q.; Li, L.; Liu, X. Assessment of Multiple Ecosystem Services and Ecological Security Pattern in Shanxi Province, China. *Int. J. Environ. Res. Public Health* **2023**, *20*, 4819. [[CrossRef](#)] [[PubMed](#)]
26. Yang, Z.; Zhan, J.; Wang, C. Coupling coordination analysis and spatiotemporal heterogeneity between sustainable development and ecosystem services in Shanxi Province, China. *Sci. Total Environ.* **2022**, *836*, 155625. [[CrossRef](#)]
27. Liang, X.; Guan, Q.; Clarke, K.C. Understanding the drivers of sustainable land expansion using a patch-generating land use simulation (PLUS) model: A case study in Wuhan, China. *Comput. Environ. Urban. Syst.* **2021**, *85*, 101569. [[CrossRef](#)]
28. Yin, L.; Wang, L.; Li, T.; Lu, S.; Yin, Z.; Liu, X.; Zheng, W. U-Net-STN: A Novel End-to-End Lake Boundary Prediction Model. *Land* **2023**, *12*, 1602. [[CrossRef](#)]
29. Ferreira, M.R.; Almeida, A.M.; Quintela-Sabaris, C.; Roque, N.; Fernandez, P.; Ribeiro, M.M. The role of littoral cliffs in the niche delimitation on a microendemic plant facing climate change. *PLoS ONE* **2021**, *16*, e0258976. [[CrossRef](#)] [[PubMed](#)]
30. Gao, L.N.; Tao, F.; Liu, R.R. Multi-scenario simulation and ecological risk analysis of land use based on the PLUS model: A case study of Nanjing. *Sustain. Cities Soc.* **2022**, *85*, 104055. [[CrossRef](#)]
31. Li, J.; Yang, D.H.; Wu, F.Z. Dynamic simulation of land use change and carbon storage assessment in Kunming City based on PLUS and InVEST models. *Bull. Soil. Water Conserv.* **2023**, *43*, 378–387. [[CrossRef](#)]
32. Yang, Y.; Liu, L.; Zhang, P.; Wu, F.; Wang, Y.; Xu, C.; Kuzyakov, Y. Large-scale ecosystem carbon stocks and their driving factors across Loess Plateau. *Carbon Neutrality* **2023**, *2*, 5. [[CrossRef](#)]
33. Zhu, G.; Liu, Y.; Shi, P.; Jia, W.; Zhou, J.; Liu, Y.; Zhao, K. Stable water isotope monitoring network of different water bodies in Shiyang River basin, a typical arid river in China. *Earth Syst. Sci. Data* **2023**, *14*, 3773–3789. [[CrossRef](#)]
34. Wang, X.Z.; Wu, J.Z.; Wu, P.X. Spatial-temporal distribution and trade-off/synergy of water conservation, soil conservation and NPP services in Loess Plateau ecosystems, 2000–2015. *J. Soil Water Conserv.* **2021**, *35*, 114–121,+128. [[CrossRef](#)]
35. Su, C.H.; Wang, Y.L. Changes and driving factors of ecosystem services in the upper reaches of the Fenhe River Basin. *Acta Ecol. Sin.* **2018**, *38*, 7886–7898.
36. Wu, B.; Quan, Q.; Yang, S.; Dong, Y. A social-ecological coupling model for evaluating the human-water relationship in basins within the Budyko framework. *J. Hydrol.* **2023**, *619*, 129361. [[CrossRef](#)]
37. Budyko, M.I. *Climate and Life*; Academic Press: New York, NY, USA, 1974. [[CrossRef](#)]
38. Zhang, L.; Dawes, W.R.; Walker, G.R. Response of mean annual evapotranspiration to vegetation changes at catchment scale. *Water Resour. Res.* **2001**, *37*, 701–708. [[CrossRef](#)]
39. Li, W.; Zhao, Z.L.; Lv, S.S. Spatial and temporal differentiation of water purification function based on InVEST model. *J. Irrig. Drain.* **2022**, *41*, 105–113. [[CrossRef](#)]
40. Ou, Y.X.; Zhu, X.; He, Q.Y. Spatial interaction between urbanization and ecosystem services: A case study of Changzhutan urban agglomeration. *Acta Ecol. Sin.* **2019**, *39*, 12. [[CrossRef](#)]
41. Ren, Z.Z.; Chen, W.J.; Kang, H.T.; Li, X.; Zhang, X.; Wang, K. Research on threshold measurement method of influencing factors of safety vulnerability in traffic-intensive waters based on SD model. *Saf. Environ. Eng.* **2023**, *30*, 9–17. [[CrossRef](#)]
42. Zhang, F.; Zhan, J.; Zhang, Q. Impacts of land use/cover change on terrestrial carbon stocks in Uganda. *Phys. Chem. Earth Parts A/B/C* **2017**, *101*, 195–203. [[CrossRef](#)]
43. Zhang, M.F.; Liu, W.X.; Wang, J.N. Scenario simulation of ecosystem service value change in Dongguan section of Shima River Basin based on Clue-S model. *Bull. Soil. Water Conserv.* **2021**, *41*, 152–160. [[CrossRef](#)]
44. Yang, J.; Xie, B.P.; Zhang, D.G. Spatial-temporal variation of carbon storage in the Yellow River Basin based on InVEST and CA-Markov models. *Chin. J. Eco-Agric.* **2021**, *29*, 1018–1029. [[CrossRef](#)]

45. Ji, Q.Q.; Pan, Q.Q.; Wu, S.R. The spatial reconstruction of “three lives” and the impact of precipitation changes on water production services in the Yellow River Basin of Shanxi Province. *Arid. Zone Res.* **2023**, *40*, 132–142. [[CrossRef](#)]
46. Peng, Y.Y.; Liu, Y.; Gao, Q.Q. Change characteristics of clouds in China in the summer of El Niño and their relationship with precipitation. *Acta Meteorol. Sin.* **2022**, *80*, 701–720. [[CrossRef](#)]
47. Yin, Z.; Liu, Z.; Liu, X.; Zheng, W.; Yin, L. Urban heat islands and their effects on thermal comfort in the US: New York and New Jersey. *Ecol. Indic.* **2023**, *154*, 110765. [[CrossRef](#)]
48. Shang, M.; Luo, J. The Tapio Decoupling Principle and Key Strategies for Changing Factors of Chinese Urban Carbon Footprint Based on Cloud Computing. *Int. J. Environ. Res. Public Health* **2021**, *18*, 2101. [[CrossRef](#)]
49. Zhang, C.L.; Zhao, J.B.; Niu, J.J. Study on Warming and Drying Climate of Shanxi Loess Plateau in Recent 50 Years. *J. Arid. Land. Resour. Environ.* **2008**, *22*, 70–74. [[CrossRef](#)]
50. Yao, Y.B.; Wang, Y.R.; Li, Y.H. Climate warming and drying of the Loess Plateau in China and its impact on the ecological environment. *Resour. Sci.* **2005**, *27*, 146–152. [[CrossRef](#)]

Disclaimer/Publisher’s Note: The statements, opinions and data contained in all publications are solely those of the individual author(s) and contributor(s) and not of MDPI and/or the editor(s). MDPI and/or the editor(s) disclaim responsibility for any injury to people or property resulting from any ideas, methods, instructions or products referred to in the content.